Rock glaciers throughout the French Alps accelerated and destabilised since 1990 as air temperatures increased

Marco Marcer, Alessandro Cicoira, Diego Cusicanqui, Xavier Bodin, Thomas Echelard, Renée Obregon, Philippe Schoeneich

communications earth & environment

ARTICLE

https://doi.org/10.1038/s43247-021-00150-6 OPEN

Rock glaciers throughout the French Alps accelerated and destabilised since 1990 as air temperatures increased

Marco Marcer[1,2,3]✉, Alessandro Cicoira[4], Diego Cusicanqui[2,5], Xavier Bodin[2], Thomas Echelard[1], Renée Obregon[1] & Philippe Schoeneich[1]

Rock glaciers—ice-rich creeping landforms typical of permafrost mountain ranges—can develop an anomalous landslide-like behaviour called destabilisation. This behaviour is characterised by failure mechanisms (including cracks and crevasses) and increases in displacement rates by one to two orders of magnitude. Existing studies of this phenomenon have been limited to a small number of landforms and short time spans. Here, we systematically investigate the evolution of rock glacier kinematics over the past seven decades for the entire French Alps by combining observations of landform features indicative of the onset of destabilisation with data on displacements rates using aerial orthoimagery. We show that rock glacier velocities have significantly increased since the 1990s, concurrent with the development of destabilisation in 18 landforms that represent 5% of the 337 active rock glaciers. This pattern of activity correlates with rising air temperatures in the region, which suggests that a warming climate may play a role in this process.

[1] Univ. Grenoble Alpes, Institut d'Urbanisme et Géographie Alpine, PACTE, Grenoble, France. [2] Univ. Savoie Mont-Blanc, CNRS, UMR CNRS 5204, EDYTEM, Le Bourget du Lac, France. [3] Technical University of Denmark, Department of Civil Engineering, Arctic DTU, Sisimiut 3911, Greenland. [4] Department of Geography, University of Zurich, Zurich, Switzerland. [5] Univ. Grenoble Alpes, CNRS, IRD Institute de Géosciences de l'Environement (IGE, UMR 5001), Grenoble, France. ✉email: marcma@byg.dtu.dk

Rock glaciers are debris landforms typical of the dry-cold mountain environment[1]. They are currently gaining interest in the context of water resource availability[2] paleoclimatology[3], and, due to their movement, potential natural hazards[4]. These landforms are generated when gravity triggers a creeping mechanism on permafrost debris slopes that possess a sufficiently high ice content to allow for internal deformations[5]. The creeping process confers to rock glaciers a typical cohesive flow morphology consisting of ridges and furrows created by compressive and tensile stresses, which are clearly distinguishable in the landscape[5,6]. The displacement rates of rock glaciers have been investigated at different scale, ranging from seasonal[7], decadal[8], centennial[9–11], and millennial[3,12,13].

Until a few decades ago, rock glacier displacement rates were thought to be limited to a few decimetres per year[12]. However, recent studies have shown that acceleration can take place, increasing the displacement rates of some landforms to up to several metres per year[14,15]. This acceleration pattern has been explained by the complex and non-linear relationship between permafrost creep, ground temperatures and local hydrological characteristics[8,16–20] . Increasing rock glacier displacement rates due to present-day climate warming, leading to increases in both ground temperature and groundwater content, is thus a phenomenon that is generally accepted by the scientific community[21–24]. In the European Alps, this climate-dependent process results in a synchronous response of rock glaciers at the regional scale, from the pluri-annual to pluridecadal temporal scales, to the point that rock glacier dynamics have been suggested as an indicator of the impact of climate change on the cryosphere[25].

In the past decades, a growing number of studies have reported anomalous rock glacier behaviour commonly addressed as 'destabilisation'[23,26–32]. Though no widely accepted definition has yet been established, rock glacier destabilisation is commonly defined as a landslide-like behaviour consisting of a sudden acceleration of part of the landform, where the displacement rates increase up to two orders of magnitude and cause of increasing strain between destabilised and non-destabilised areas (see Fig. 1). Such a phase can last from a few years to several decades, usually ending with a sudden deceleration or inactivation of the landform[29,33]. Exceptionally, a structural collapse of the landform may also occur[27]. Destabilisation onset is also characterised by the development of specific morphological features on the rock glacier surface (i.e. crevasses, cracks, and scarps), generally interpreted as 'destabilisation signs' (Fig. 2). These features most likely play a crucial role in the destabilisation process as they increase the thermal exchange with the atmosphere and allow an abundant infiltration of meteoric water and meltwater into the landform, thus reducing the shear resistance of the permafrost material and boosting the landslide-like behaviour. Thus, positive feedback develops between the acceleration and development of destabilisation signs, which, once initiated, can be assumed to compromise the rock glacier dynamics[16]. The destabilisation signs mostly develop in steep and convex areas, where extending flow occurs. Although this topographical predisposition is critical to the destabilisation onset[29,34], destabilisation does not occur for all rock glaciers presenting a high topographical predisposition[34]. This suggests that other geotechnical factors (e.g. the internal structure of a rock glacier, the debris granulometry, temperature, hydrology, and the stress conditions related to the overloading input of rock mass) also control the onset of the destabilisation process[17,29,35]. Once the process is triggered, the landform becomes dynamically discontinuous since the areas downslope from the destabilisation signs develop a dynamic behaviour that is different from that of the upslope areas. In particular, the acceleration of the downslope areas is generally higher, whereas the behaviour of the upslope part of the rock glacier remains unchanged.

Studies suggest that destabilisation may result from external mechanical loading[29,32] or climatic forcing[23,30,31]. According to the mechanical loading hypothesis, destabilisation is triggered by the phenomena that induce variations in the rock glacier's internal stress regime, such as external loading caused by a rockfall on the rock glacier surface or the passage of a thick area of the rock

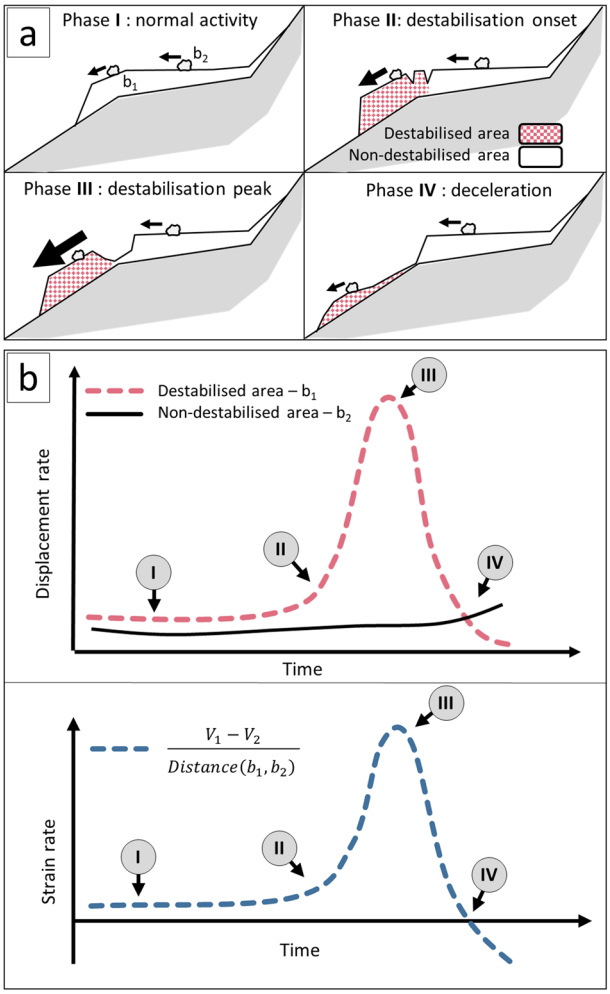

Fig. 1 Rock glacier destabilization process. Conceptual representation of the destabilisation process in terms of the geomorphological (**a**) and dynamic (**b**) evolution of the areas upslope (non-destabilised area) and downslope (destabilised area) from the surface disturbances. The dynamic behaviour of the rock glacier is described by the displacement rates evaluated on boulders of the destabilised (boulder b_1) and non-destabilised (boulder b_2) of the rock glacier, and by strain rate, i.e. the mechanical tension at the landform surface evaluated as the difference between the displacement rates of b_1 and b_2, divided by their distance. A non-destabilised rock glacier is characterised by homogeneous displacement rates in both areas that generate low strain rates (Phase I). The destabilisation onset is characterised by the development of surface disturbances (Phase II), which accelerates significantly in the downslope area, while the upslope area does not destabilise, causing increasing strain. The displacement rates of the downslope area and surface strain reach their maximum (Phase III) within a few years/decades after the destabilisation onset, creating a larger discontinuity between upslope and downslope velocities. After the peak phase (III), the destabilised area decelerates because of mass loss and/or flatter topography (Phase IV) and reaches inactivation.

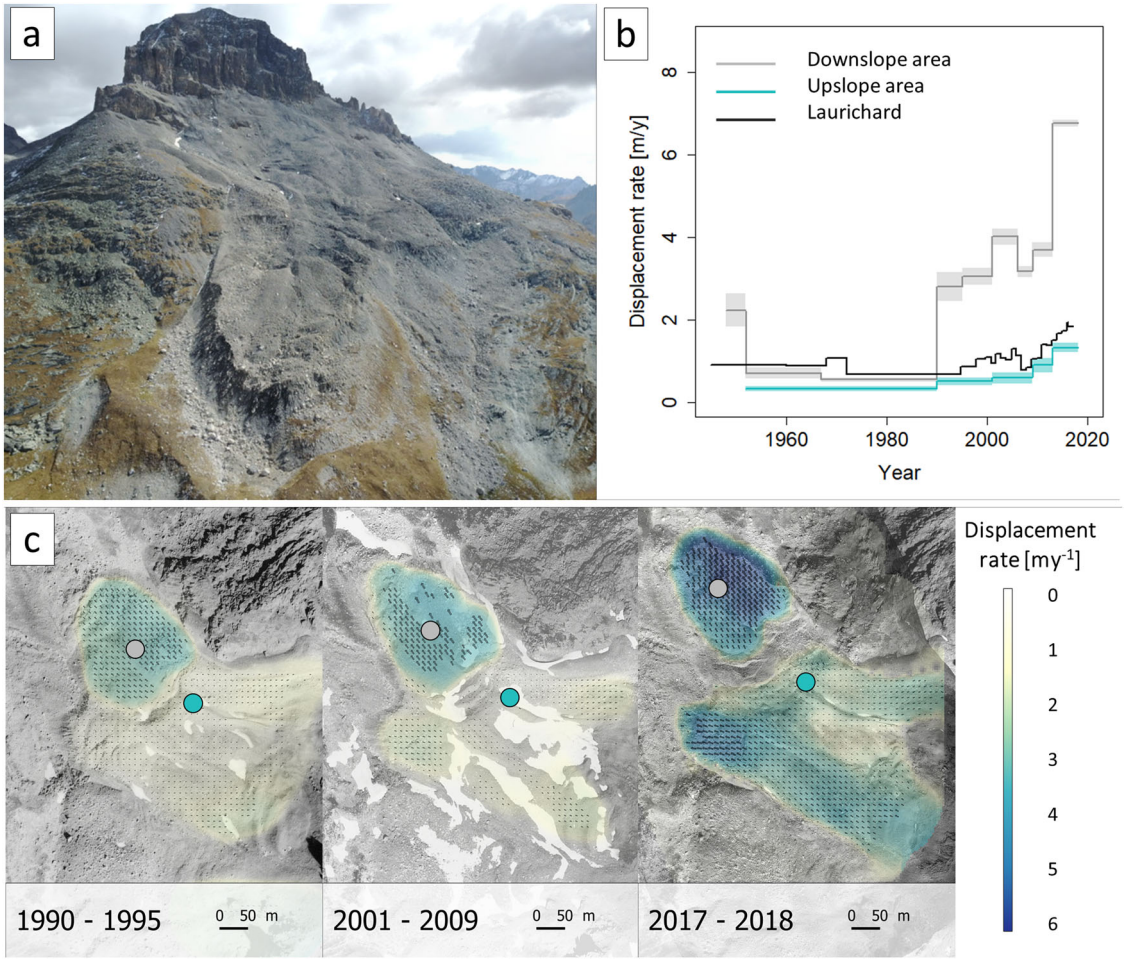

Fig. 2 Destabilisation example at the study site of Pierre Brune (PB). PB is a destabilised rock glacier (**a**) approaching the peak phase (Phase II to III in Fig. 1). More detailed analysis is provided for PB in Supplementary note 2. Similar results are produced for every site in this study and are available in the Supplementary information. Displacement rates are plotted with the movements of the Laurichard (La) rock glacier for comparison with a non-destabilized landform (**b**). Destabilisation onsets between 1990 and 1995 in relation to the fast development of crevasses (**c**). A crevasse was already visible in the area in 1990 and belongs to an earlier destabilisation phase that occurred during the late 1940s. The destabilised mass starts moving faster than the upslope areas, creating a strongly discontinuous deformation pattern and the landform is dynamically disconnected in correspondence of the surface disturbances. While the upslope area presents a behaviour similar to the Laurichard rock glacier (non-destabilised), the downslope mass is still accelerating and reaching much higher displacement rates. © IGN.

glacier over a steeper section. This hypothesis is supported by several observational studies that report destabilisation onset after the occurrence of such phenomena[29,32]. The climatic forcing hypothesis purports that destabilisation is provoked by climate change. In this case, increasing air temperatures are responsible for permafrost degradation (i.e. permafrost warming, interstitial ice thaw, and increasing water content), making the landform velocity more sensitive to temperature[17,19,22,36,37] (and decreasing the mechanical resistance of the debris-ice mixture[21,35]. Degrading permafrost is more prone to fracturing and the development of openings (i.e. destabilisation signs) in the rock glacier surface[35,38]. These openings enhance permafrost degradation by modifying local hydrology, establishing a positive feedback process that can compromise landform stability[35]. Both of these hypotheses—external mechanical loading and climatic forcing—are based on a limited number of case studies, and it is challenging to identify the main controlling factors in destabilisation.

Although some researchers have investigated patterns and trends in the displacement rates of rock glaciers at a regional scale[14,39,40], no similar investigations have yet focussed on destabilisation. In the present study, we aim to fill this research void and provide a valuable tool to the mountain permafrost community via a systematic regional-scale analysis of rock glacier displacement rates and destabilisation onset over the past seven decades. The region we chose for this study is the French Alps, i.e. the surface of the European Alps within the French national borders. These mountains are rich in rock glaciers with many potentially destabilised landforms[34,41]. In the same study region, Marcer et al.[34] classified all the creeping rock glaciers were classified into five 'destabilisation rate' categories according to their geomorphological characteristics. This study indicated that 10% (46) of the creeping rock glaciers in the French Alps show potential destabilisation (Fig. 3), therefore providing an opportunity to investigate the destabilisation process on a larger scale than that of previous studies.

Here we combine the geomorphological observations provided by Marcer et al.[34] with an analysis of the horizontal displacement rates of landforms over the past seven decades, using manual feature tracking on aerial orthoimagery. This analysis consisted of three steps: (1) regional-scale assessment; (2) site-scale analysis, and; (3) statistical analysis of the links to climatic conditions. Accounting for the various spatial and temporal scales of the

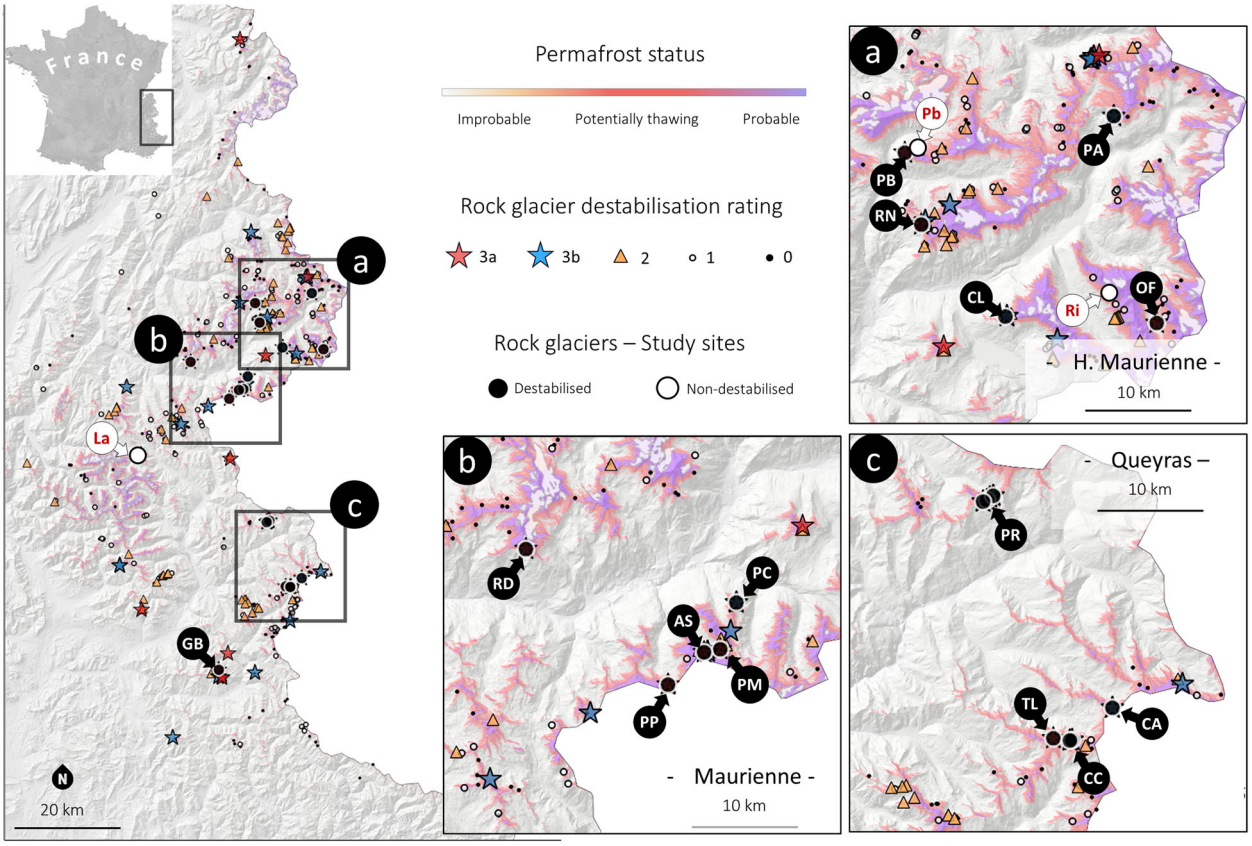

Fig. 3 Study region summary. French Alps: permafrost status and localization of active rock glaciers rated by geomorphological evidence of destabilisation[34]. Most of destabilized landforms occur in the Haute-Maurienne (**a**), Maurienne (**b**) and Queyras (**c**) areas. Destabilisation rates vary from 0 (no geomorphological evidence of destabilisation) to 3 (evidence of developing surface disturbances and consequent dynamic discontinuity in the landform). In Rate 3a, the surface disturbances are characteristic of more severe destabilisation, i.e., crevasses and scarps, while in Rate 3b only shallow cracks are observed. Rates are 1 and 2 are intermediary, corresponding respectively to non-destabilised and developing surface disturbances. Rock glaciers with a destabilisation rate of 3 and found by this study to have displacement rates above 3 my^{-1} are classified as destabilised and investigated in detail. The rock glaciers investigated in this study are designated by an acronym; CL: Col du Lou, PB: Pierre Brune, RN: Roc Noir, PM: Pierre Minieu, PP: Pointe Paumont, TL: Tête de Longet, GB: Grand Bérard, PC: Pointe du Clot, OF: Ouille du Favre, PA:Pointe des Arses, AS: Aiguille Scolette, PR1: Petite Rochebrune 1, PR2: Petite Rochebrune 2, PR3: Petite Rochebrune 3, RD: Rocher des Dents, CA: Pic Caramantran, CC1: Crête du Coq 1, CC2: Crête du Coq 2, La: Laurichard, Pb: Pierre Blanche, Rib: Ribbon. © IGN.

investigation, and the expected accuracy of the results, the combination of methods employed in our study represents the best trade-off between existing techniques and data availability. To ensure valid interpretations and fruitful discussions, we carefully verified the reliability of these approaches.

In Step 1, we first estimated the displacement rates of all active rock glaciers via manual feature tracking of moving boulders on four orthomosaics provided by the French National Institute of Geography (IGN). These four orthomosaics result from the assemblage of orthoimages acquired during different periods: (i) 1948 to 1952, (ii) 2001 to 2004, (iii) 2008 to 2009, and (iv) 2015 to 2017, and allow us to compute displacement rates over three time periods:

- Period 1 from 1948–1952 to 2001–2004;
- Period 2 from 2001–2004 to 2008–2009;
- Period 3 from 2008–2009 to 2015–2017.

This analysis provides a rough estimation of the rock glacier dynamics in the region and their spatio-temporal evolution. Most importantly, it also identifies the destabilised rock glaciers, i.e. those presenting abnormally high displacement rates (>3 my^{-1}) and signs of destabilisation development (see Fig. 3 for the study site locations; for a detailed site description of each landform, see the Supplementary information sections 1–15).

In Step 2, we performed a detailed analysis of the displacement rates and geomorphological evolution of these destabilised landforms. We also investigated three rock glaciers not presenting destabilisation (hereafter referred to as 'non-destabilised') to obtain displacement evolution rates that could be compared to the destabilised landforms. In this local-scale analysis, we used a higher number of orthoimages, specifically computed from aerial (IGN) and Unmanned Aerial Vehicle (UAV) photogrammetry. To generate the orthoimages for each site, we used the Structure from Motion approach[42], here integrated into Agisoft Photoscan software. We used aerial imagery acquired by the IGN since the 40s at a plurennial frequency (generally, five to fifteen years) and recent UAV surveys conducted by our team. We also used the orthoimages to compute the surface velocity and strain rate fields, and explore the possible mechanical drivers of crevasses at the local sites, as has been done in glaciological studies[43]. For the destabilised rock glaciers, we calculated the strain rates between non-destabilised and destabilised areas. For non-destabilised rock glaciers, we evaluated the strain rates between the available upper and lower moving targets.

In Step 3, to explore the hypothesis of a statistically significant correlation between climate and destabilisation, we conducted an analysis of the link between this phenomenon and climate changes. In particular, we evaluated the correlation significance

between the dynamic evolution of both destabilised and non-destabilised rock glaciers and the evolution of air temperature anomalies—extracted for each rock glacier site using the SAFRAN (Système d'Analyse Fournissant des Renseignements Atmosphériques à la Neige) meteorological reanalysis[44] and HISTALP (Historical Instrumental climatological Surface Time series of the greater Alpine region) database[45]. Our aim was to further contribute to the understanding of these processes of rock glacier destabilisation.

Results

Regional-scale assessment. For 337 rock glaciers, we evaluated significant displacement rates in at least one of the three periods considered (see above for period definitions), and for 114 rock glaciers, we obtained substantial movements in all three periods (Fig. 3). Incomplete displacement rate sets were mostly due to insufficient image quality in one or more frames, sometimes resulting in movements below the detectability thresholds. Because these thresholds are inversely proportional to the duration of the time period, slow rock glaciers are more easily detectable over longer time periods. On average, in our data set, only rock glaciers moving faster than 0.52 my^{-1} could be detected in Period 3. In Period 1, this threshold was 0.10 my^{-1}. We did not use incomplete displacement rate sets for the statistical consideration below.

Our results show an increase in rock glacier displacement rates in the French Alps over the past seven decades (Fig. 4, Table 1). Mean displacement rates increased from 0.42 my^{-1} (Period 1) to 1.09 my^{-1} (Period 2) to 1.44 my^{-1} (Period 3). Most of the acceleration occurred between Period 1 and Period 2 (average absolute increase of 159%, average relative increase of 192%), while between Period 2 and Period 3, the acceleration was significantly lower (average absolute increase of 32%, average relative increase of 30%). For 97 rock glaciers, we observed a significant increase in displacement rates from Period 1 to Period 2, while only two landforms show significantly decreased displacement rates. From Period 2 to Period 3, we observed increasing displacement rates for 40 landforms, and deceleration for 18 landforms.

A comparison of displacement and destabilisation rates proposed by Marcer et al.[34] indicates that landforms developing geomorphological evidence of destabilisation show, on average, three to five times higher displacement rates than landforms not developing such features (Fig. 5, Table 1). Although the geomorphological characteristics of rock glaciers are linked to their dynamic behaviour, about half of the potentially destabilised rock glaciers (Rates 3b and 3a) showed displacement rates below 2 my^{-1} in Period 3 (Figs. 4 and 5). In total, during Period 3, 18 rock glaciers show both destabilisation signs and displacement rates above 3 my^{-1} and are, therefore, identified as destabilised. Their average displacement rates increased from 0.69 my^{-1} in Period 1 to 4.55 my^{-1} in Period 3.

Site-scale analysis. We conducted a detailed analysis of the eighteen destabilised rock glaciers and three non-destabilised rock glaciers identified in the region at the site-scale. The rock glaciers investigated in this study are designated by an acronym (see Fig. 3 for geographic overview and acronym meaning).

The three non-destabilised rock glaciers (Pb, La, Rib) show two distinct displacement rate phases: low displacement rates in the 1950–90 period and gradual acceleration over the following thirty years. Although they all follow a similar general trend, individual sites show significant differences. For the Pb rock glacier, we also observed high displacement rates in the late 40s, before the low-velocity phase. Among the non-destabilised rock glaciers, we observed the highest velocity on the Northern lobe of the Rib rock glacier (2.5 ± 0.2 my^{-1}) during the 2009–2013 period. We used the displacement rates for the La (Laurichard) rock glacier as a reference for comparisons between different landforms (Fig. 2) due to the outstanding long-term series of geodetic measurements of surface targets made since 1982[8,46,47] and its coherence with the regional-scale trend observed in the European Alps[39] .

The eighteen destabilised rock glaciers show a pattern similar to that of the non-destabilised sites, with low displacement rates from the 1950s to 1990s and acceleration afterwards. In particular, we observed no destabilisations over these four decades. Two destabilised landforms (rock glaciers PM and PB) developed signs of destabilisation and higher displacement rates already in the late 40s, reaching 3.8 ± 0.5 my^{-1} in PB (period 1948–1952—Supplementary Fig. 5). However, these two rock glaciers did not enter a destabilisation phase, but instead remained in a secondary creep state for the following four decades. Starting in 1990, morphological signs of destabilisation preceded the abrupt acceleration of all the eighteen destabilised landforms. Five rock glaciers entered the destabilisation phase before 2000 (rock glaciers PB, RN, GB, PP, PC—see Supplementary Figs. 5, 9, 19, 21, 23), ten between 2000 and 2010 (rock glaciers TL, PM, PA, PR1, PR2, PR3, RD, CA, CC1, CC2—see Supplementary Figs. 15, 17, 27, 30, 31, 32, 34) and only three after 2010 (rock glaciers CL, OF, AS—see Supplementary Figs. 2, 24, 29). We observed deceleration (Phase IV, Fig. 1) in the TL, PP, and RN rock glaciers only, indicating that most of the destabilised landforms in the region did not peak in the destabilisation process (Phase III, Fig. 1) during the 2013–2018 period. The maximum displacement rate occurred between 2013 and 2015 on the TL rock glacier, reaching 22.1 ± 0.3 my^{-1} before a strong deceleration (Supplementary Fig. 14). We also observed exceptionally high displacement rates on the RD (15.2 ± 0.3 my^{-1} in 2013–2016—Supplementary Fig. 31) and PC (9.7 ± 0.2 my^{-1} in 2013–2016 my^{-1}—Supplementary Fig. 23) rock glaciers, while the other landforms present maximum velocities usually between 4 and 6 my^{-1}.

The destabilisation onset patterns vary for the different sites. For most sites, displacement rates increased gradually through the 1990s and 2000s, concurrently with the development of increasingly severe destabilisation signs. In contrast, other sites exhibit an abrupt transition to the destabilisation phase, marked by a strong acceleration and the sudden development of severe destabilisation signs. The velocity of the AS rock glacier, for example, sharply increases from 1.3 ± 0.4 my^{-1} in 2009–2013 to 6.5 ± 0.4 my^{-1} in 2013–2016, in parallel with the rapid development of a large crevasse sectioning the landform across its entire width (Supplementary Figs. 28, 29). We observed similar phenomena for the PB, RN, TL, OF and RD rock glaciers (Supplementary Figs. 13, 31, 24, 8, 4). The destabilisation of the PB rock glacier, for example, occurs as an abrupt increase in displacement rates from 1990 to 1995, concurrently to the development of three crevasses on the landform surface. In the following two decades, however, we observed no acceleration, and it was only in 2013–2017 that the landform experienced a second destabilisation phase concomitant to the development of a new series of crevasses and significant acceleration (Fig. 5).

Since crevassing could be a critical process in the destabilisation of rock glaciers, we calculated strain rates for eight destabilised rock glaciers before and after crevasse development by differentiating the displacement rates of boulders between the higher and the lower (destabilised) area. In general, we found that destabilisation onset and the appearance of surface disturbances correspond to a critical strain rate of roughly $10^{-2}\,y^{-1}$. In comparison, our calculation of the strain rates of non-destabilised rock glaciers showed that they were one order of magnitude lower

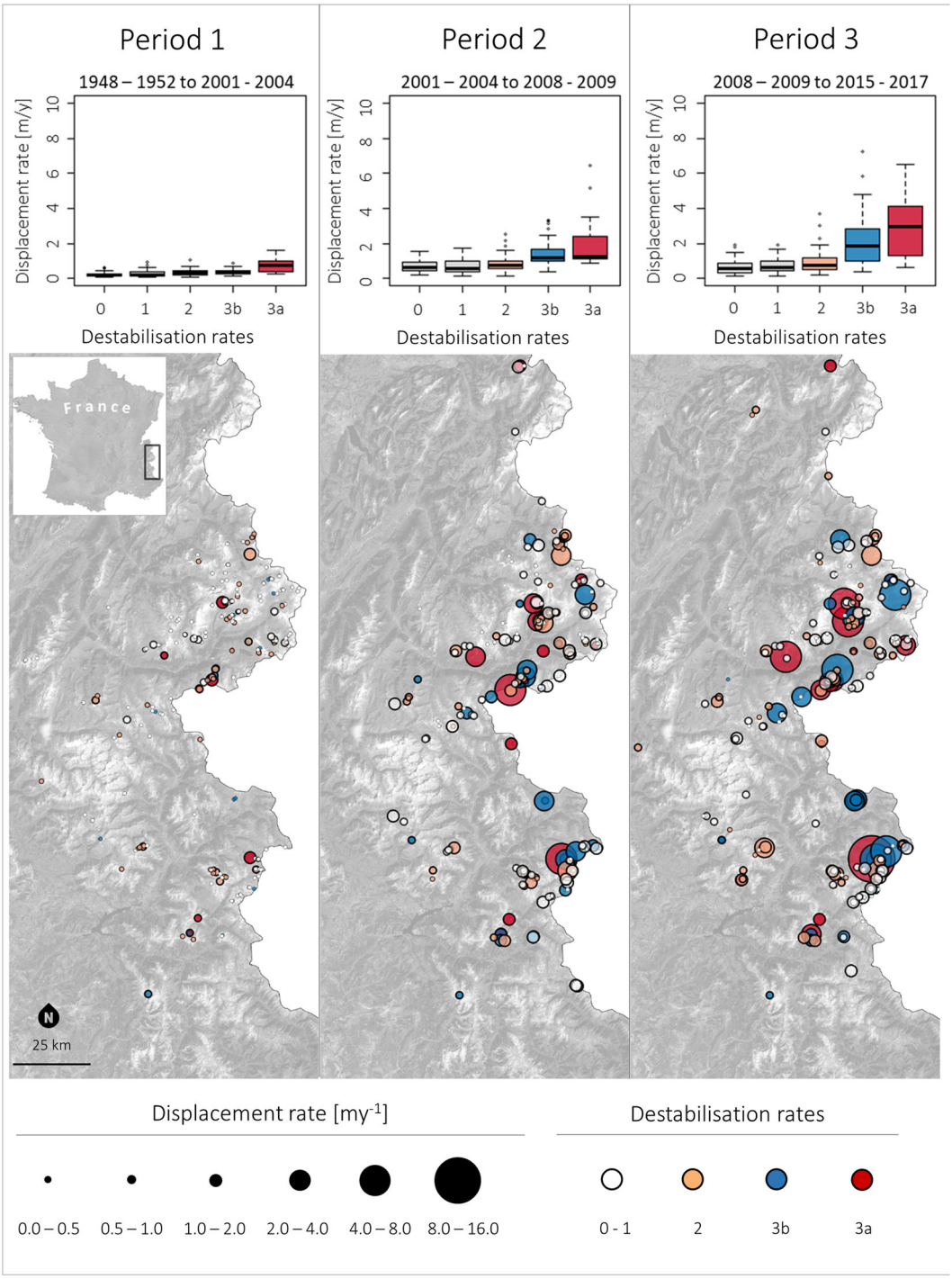

Fig. 4 Rock glacier displacement rates evolution. Evolution of the rock glacier displacement rates in the French Alps in the three periods investigated and grouped by destabilisation rate. The symbol size is proportional to the measured displacement rate, while the symbol colour is assigned according to the destabilisation rate (see Fig. 3 for rate description). The boxplot respect the standardized sizes: the interquartile (IQR) range groups observations from the 25th (Q1) to 75th (Q3) percentile, while the whiskers represent the maximum (Q3 + 1.5*IQR) and minimum (Q1−1.5*IQR). © IGN.

(Fig. 6). A *t*-test shows no statistical difference between strain rates of non-destabilised rock glaciers and rock glaciers before the onset of destabilisation. On the other hand, we noticed that the critical strain rate for rock glacier destabilisation is consistent with the crevassing values on Alpine glaciers, ranging from 10^{-2} to $10^{-1}\,y^{-1}$ for ice temperatures comprised between −10 °C and 0 °C[48]. Most of the apparent variation in the observed critical strain rates of Alpine glaciers can be attributed to variations in the ice properties, most of which are linked to ice temperature. For rock glaciers, variations in the volumetric ice content could be of equal importance. However, a given strain rate is not equivalent to a single unique combination of cartesian stresses, which also depend on the geometry of the landform[49]. In comparison to critical strain rates, critical stresses could provide a more robust criterion for fracture onset. However, neither the ground temperature nor the internal deformation profiles are known for the investigated set of rock glaciers, and more specific studies are required to constrain the calculation of their stress regime.

Table 1 Summary of regional scale displacement rates.

	Mean displacement rate [my^{-1}]			Relative increase in displacement rate [%]	
Dest. rate	Period 1	Period 2	Period 3	Period 1 to Period 2	Period 2 to Period 3
0	0.22	0.72	0.73	227	1
1	0.27	0.71	0.77	163	8
2	0.35	0.85	1.02	143	20
3b	0.39	1.46	2.36	274	62
3a	0.77	2.18	3.45	183	58
Mean	0.3	0.97	1.25	223	29

Regional-scale displacement rates and relative increase in displacement rate (in %) by period and destabilisation rates. Period 1: from 1948–1952 to 2001–2004; Period 2: from 2001–2004 to 2008–2009; Period 3: from 2008–2009 to 2015–2017. Destabilisation rates[34] characterise the landforms from their geomorphological evidence of destabilisation. Rock glaciers with lower rates do not show significant evidence of destabilisation, while higher rates are attributed to rock glaciers developing mild (Rate 3b) or severe (3a) destabilisation signs, causing dynamic discontinuity in the landform.

Statistical analysis. Our statistical results demonstrate that rock glacier displacement rates correlate with the mean annual air temperature (MAAT, Fig. 7). This correlation is stronger for the displacement rate logarithm, indicating an exponential relationship between air temperature and displacement rates. For all the active rock glaciers in the region, the correlation coefficients range from $R^2 = 0.21$ for non-destabilised rock glaciers to $R^2 = 0.55$ for destabilised landforms. The regression coefficients are always statistically significant (p-value < 0.01), rejecting the null hypothesis that the predictor variable (air temperature) does not affect the response variable (rock glacier displacement rates). Also at the site-scale, the correlation between MAAT and displacement rates for destabilised ($R^2 = 0.54$, p-value<0.01) and non-destabilised rock glaciers ($R^2 = 0.14$, p-value < 0.1) is statistically significant. Concerning the destabilisation onset, air temperature anomaly is also found to be a 'very good'[50] (area under the curve, AUC = 0.82,) discriminator of the transition between the non-destabilised and destabilised phases of the local sites.

Discussion

As in previous studies[40], our results indicate a regional-scale increase in rock glacier displacement rates in the past seven decades, which developed relatively synchronously within two decades. Overall, ~5% of the region's total active rock glaciers show destabilisation, which mostly developed since the late 1990s, concomitant to the regional-scale rock glacier acceleration. Destabilisation, combining morphological indicators and an acceleration phase, affects about 40% of the rock glaciers showing destabilisation signs[34]. This indicates that cracks, crevasses, and scarps may form in rock glaciers with low displacement rates and that they are not necessarily followed by the strong acceleration typical of the destabilisation process. Nevertheless, we observed that the destabilisation signs can precede a (delayed) future acceleration for the rock glaciers that have not yet undergone destabilisation. In our study area, we observed this phenomenon for the PB and PM rock glaciers; while these glaciers have shown destabilisation signs since the 1940s, they entered the destabilisation process only five decades later. In this sense, local geotechnical characteristics and the landform's internal structure are considered fundamental for the onset and development of rock glacier destabilisation[34]. While local topography creates extending flow patterns that increase the tensile stresses to a critical value, the geotechnical characteristics of rock glaciers—determined by lithology, internal structure, ice/water contents, and perhaps external loading—determine their resilience to temperature variations and mechanical stress and, ultimately, to the destabilisation trigger[35]. Once the destabilisation process is triggered, displacement rates display significant variability from site to site. The highest displacement rates may depend on the geometrical characteristics (such as thickness and slope angle) of the destabilised section, as well as underground water circulation[23,33,51]. The temporal development of the destabilisation phase is also variable, as shown by the sites that have already passed the acceleration phase and are now decreasing their velocity, while others are still accelerating.

We determined that the evolution of the displacement rates is statistically correlated to air temperature, which is consistent with the fact that air warming trends cause a generalised rock glacier acceleration due to non-linear feedbacks in their hydrology and thermal regime[14,15,20,,51]. As already mentioned, two sites (rock glaciers PB and PM) showed evidence of an earlier destabilisation phase in the 1940–1950 period, while five sites have significantly higher displacement rates in the 1940–1970 period than in the 1980–1990 period (rock glaciers RN, OF, CA, GB and PR1). This phenomenon, also observed at other sites in Switzerland (Graben Gufer and Gugla rock glaciers[23]) and Austria (Hinteres Langtalkar rock glacier[26]), roughly coincides with the reported rock glacier acceleration linked to the air temperature increase that occurred during the early 40s[52]. This temporal pattern in rock glacier destabilisation and displacement rates is also similar to the mass balance pattern of the glaciers in the region, which, during the 20th century, was observed to be negative in the 40s to 50s and 80s to the present[53–55].

Overall, our results indicate that increasing air temperature is necessary for destabilisation onset, while proper geotechnical characteristics and topography are required preconditions. Increasing air temperature is known to be responsible for permafrost warming at a global scale[56], which can then decrease the mechanical resistance of the permafrost material constituting rock glaciers. Air temperature exerts a strong non-linear influence (directly and indirectly) on rock glacier creep, which can be physically summarised with a power-law equation[20–22]. The consequent variations in rock glacier dynamics can also facilitate the development of surface openings in extending flow areas, which can then increase the permeability of the rock glacier to surface water and external temperature, engaging the positive feedback of landform degradation described by previous studies[16,35]. In this sense, the exponential correlation between displacement rates and air temperature anomalies at destabilised rock glacier sites suggests a process of permafrost degradation, which may trigger a destabilisation phase, depending on local geotechnical conditions. Air temperature control of the dynamics of destabilised rock glaciers seems weaker in longer time-scales, as rock glaciers eventually encounter deceleration (Phase IV, Fig. 1) despite further air temperature increase. Temperature increase can therefore be considered as a necessary but insufficient factor for destabilisation onset at the regional scale, but it loses its control over local-scale dynamics after destabilisation occurs and local site characteristics become dominant. In several studies[23,30,31], climate warming has already been hypothesized as a potential cause for rock glacier destabilisation, and the present investigation contributes new evidence supporting this hypothesis. Our results strongly suggest that rock glacier destabilisation should be investigated as a large-scale phenomenon of climate-induced degradation of the cryosphere.

Methods

This study is based on the analysis of surface displacement rates, destabilisation occurrences and their correlation with climate, evaluated using a statistical approach.

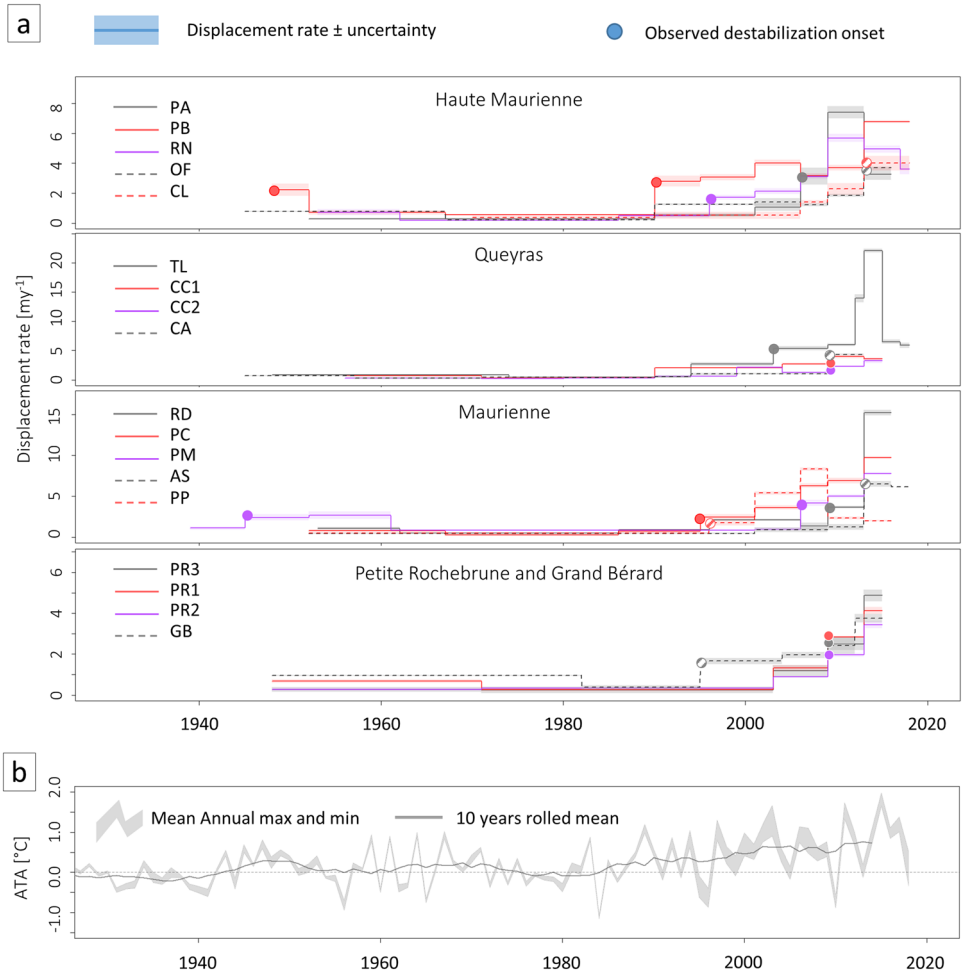

Fig. 5 Evolution of the displacement rates of destabilised rock glaciers. On panel **a** are presented the displacement rates of destabilized rock glaciers grouped by geographical regions. The dots on the displacement rate graphs indicate the observed onset of the destabilised phase. The rock glaciers presented are designated by an acronym; CL: Col du Lou, PB: Pierre Brune, RN: Roc Noir, PM: Pierre Minieu, PP: Pointe Paumont, TL: Tête de Longet, GB: Grand Bérard, PC: Pointe du Clot, OF: Ouille du Favre, PA: Pointe des Arses, AS: Aiguille Scolette, PR1: Petite Rochebrune 1, PR2: Petite Rochebrune 2, PR3: Petite Rochebrune 3, RD: Rocher des Dents, CA: Pic Caramantran, CC1: Crête du Coq 1, CC2: Crête du Coq 2. On panel **b** is presented the mean annual air temperature anomaly in the period 1850–2018 for the whole French Alps.

Statistical analysis. The correlation between mean air temperatures (predictor variable) and displacement rates during the same period (response variable) is estimated at first using a linear regression model, weighting each observation proportionally to the duration of the period covered. The performance of the regression model is evaluated using the correlation coefficient R^2 and the statistical significance of the correlation is evaluated using the p-value. In addition to linear regression, logistic regression is used to quantify the discriminative power of mean air temperature in destabilisation occurrence. For each local site, displacement rate periods are classified into a binary response variable depending on their belonging to either a non-destabilised phase (see Phase I in Fig. 1) or a destabilised phase (see Phases II, III, and IV in Fig. 1). The transition from Phase I to Phase II is determined for each site when the development of destabilisation signs is first observable (Fig. 5). Mean air temperatures for each period are computed and used as a predictor variable for the rock glacier phase in a logistic regression model. Model quality is evaluated using the AUC, measuring the discriminatory ability of air temperature on the transition of the rock glaciers from stability to destabilisation[50].

Rock glacier displacement rates. The displacement rates are estimated by diachronic orthoimage comparisons[57] for both the local- and regional-scale analyses. Two steps are performed for each available orthoimage pair: (i) manual tracking of rock glacier surface features to compute displacement rates, and (ii) definition of stable areas for uncertainty assessment. The methodological difference between the local- and regional-scale assessments lies in the number of moving targets and stable areas used in the analysis, which are higher in the local-scale assessment. The aim of this was to work with a reasonable trade-off between effort and study goals with the goal of obtaining a general regional context of rock glacier displacement rates to contextualise the more detailed results obtained by the local-scale analysis. Some of the destabilised sites benefit from an additional analysis consisting of (iii) automatic feature tracking of high resolution orthoimages, allowing spatial calculation of distributed 2-dimensional displacement rate fields.

Manual feature tracking. Surface displacements were measured by tracking boulders clearly identifiable in all available frames. The displacement rates were then computed by dividing the distance covered by the boulders by the time elapsed between two frames. In the regional-scale analysis, only one boulder, located in the area qualitatively showing largest displacements, was tracked and used to compute displacement rates. In the site-scale analysis, at least two boulders located upslope and downslope the surface disturbances are tracked in order to observe the displacement rate evolution of different landform areas. The fastest-moving boulder is used in the statistical analysis.

The suitability of the one-boulder approach used in the regional-scale analysis was assessed by comparing the data obtained with the displacement rates evaluated at the local sites on multiple boulders. On a sample of 48 displacement rates, we observed good agreement between the displacement rates evaluated from regional- and local-scale analysis ($R^2 = 0.96$, median error $= 0.19$ my^{-1}), suggesting that the one-boulder approach is a valid first-order approximation of rock glacier maximum displacement rates.

Uncertainty assessment. Using orthoimage pairs to evaluate displacement rates involves a source of uncertainty linked to the errors in the orthoimages used for the surface feature tracking process. The main source of uncertainty is due to local distortions of orthoimages. To account for this source of uncertainty, stable areas (e.g. bedrock, vegetated patterns) are identified in different orthoimages and their relative movements are then used to quantify the uncertainty in displacement rate assessments due to local distortions.

Uncertainty assessment in the regional-scale analysis was performed by identifying only one stable area per investigated landform, providing the displacement rate uncertainty for each orthoimage pair. To ensure that we do not identify apparent movements as true rock glacier displacements, we applied a safety factor equal to two to the uncertainty estimation. This means that rock glacier movements that were lower than twice the apparent movement in the stable area were considered as not significant and discarded. In the local-scale analysis, four to ten stable areas were identified, depending on the study site. The displacement rate uncertainty was then computed for each moving target by using a mean function linearly weighted on the distance between the moving target and the available stable area apparent movements.

The suitability of the one stable area per landform approach was assessed by comparing uncertainties issued from regional- and local-scale analyses. The assessment shows that the approach used at the regional scale is suitable as the uncertainty produced is of the same order of magnitude as those computed using the local-scale approach. In particular, the results indicate that, after applying the safety factor, 46 out of 47 uncertainty estimations are higher in the regional-scale analysis than in the local-scale analysis, showing that we are unlikely to consider apparent movements on rock glaciers as significant displacements.

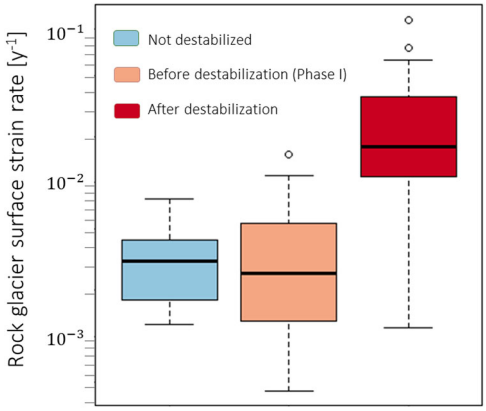

Fig. 6 Rock glacier surface strain rates measured at the local sites. The strain rate is measured as a variation of displacement rates (my^{-1}) over the distance between the two points projected on the central flow axis. This is done for each period where displacement rate pairs were available on the orthoimages. Low strain rate values in destabilised rock glaciers refer to the deceleration of the destabilised area (Phase IV—Fig. 1). The boxplot respect the standardized sizes: the interquartile (IQR) range groups observations from the 25th (Q1) to 75th (Q3) percentile, while the whiskers represent the maximum (Q3 + 1.5*IQR) and minimum (Q1−1.5*IQR).

Spatial distribution of displacement rates. For local site analyses and where high quality aerial images are available, the spatial distribution of the displacement rates was computed using the IMCORR algorithm. The software output consisted of a point grid of estimated displacements and directions. After manual filtering of output errors (e.g. unrealistic displacements due to shading and/or snow), the point grid was interpolated using the inverse distance weighted method to produce a displacement rate heatmap (Supplementary Figs.1, 6, 10, 15, 17).

Data

Climatic data. Climate is identified as the air temperature anomaly since the end of the preindustrial era (i.e. 1850) and it is evaluated at each rock glacier location using climate datasets for the French Alps. For the 1958–2018 period, data are extracted from the SAFRAN reanalysis, which operates for 23 massifs in the French Alps, and within which atmospheric conditions, in particular temperature, are assumed to be homogeneous and vary with elevation using 300 m elevation steps[44]. For earlier periods, the HISTALP gridded data (1 km cell) were used. They consist of an interpolation of weather station data in the European Alps since 1780[45]. To combine these two data sets, the overlapping period between SAFRAN and HISTALP data (1958–2014) was used to compute a linear model to extrapolate the SAFRAN data in the past from 1850 to 1957. The correlation coefficient between

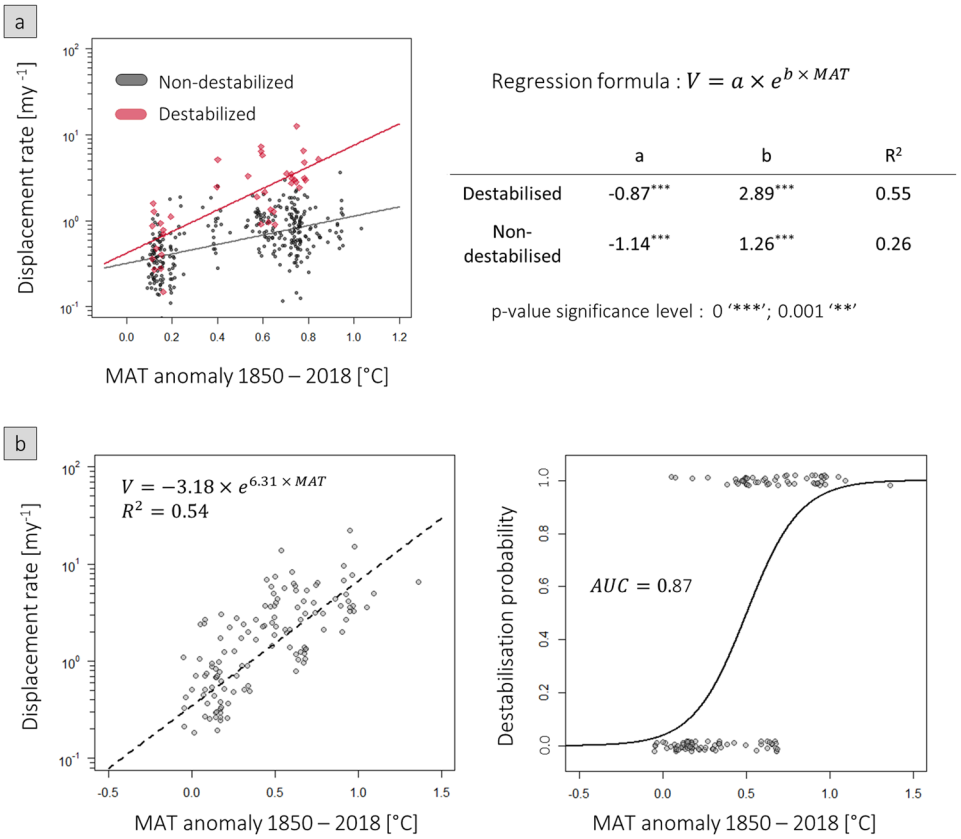

	a	b	R^2
Destabilised	-0.87***	2.89***	0.55
Non-destabilised	-1.14***	1.26***	0.26

p-value significance level : 0 '***'; 0.001 '**'

Fig. 7 Correlations between displacement rates and air temperature. Statistical analysis of the correlation between mean air temperature (MAT) anomalies since the preindustrial period and rock glacier displacement rates at the regional (**a**) and site (**b**) scales. For the regional-scale analysis, the relation between the MAT anomaly and the displacement rates is modelled for both non-destabilised and destabilised rock glaciers, and the regression coefficients are presented in the table. For the site-scale analysis, linear and logistic regressions are evaluated on the aggregated measures for all sites.

the two data sets (SAFRAN and HISTALP) varies from 0.4 to 0.9, depending on the rock glacier site.

Displacement rates. The displacement rate analysis is based on orthoimages originating from three sources: (i) orthomosaics produced by the National Institute of Geography (IGN) for the entire French territory, (ii) local orthoimages produced using aerial images acquired by the IGN photogrammetric missions since the late 40s, and (iii) local orthoimages produced using in-situ UAV photogrammetry, performed in 2017 and 2018. The regional-scale analysis was based only on the first data source, while the local-scale analysis benefits from the second data source as well. UAV photogrammetry was conducted only on four destabilised rock glaciers (PB, RN, CL and TL). For a summary of available orthoimages and their characteristics used in the local-scale assessment, see the supplementary materials.

The orthoimosaics provided by the IGN consist of assembled orthoimages of each administrative department collected over a specific time period. The orthoimages in an orthomosaic can, therefore, be collected in different years. The Supplementary materials provide a synthesis of orthoimage dates per administrative department. The advantage of this data source is that it is ready-to-use data at relatively high quality at the regional scale. This allows to focus on gathering displacement rate data rather than producing orthoimages at the regional scale. For each rock glacier in the region, four orthomosaics for the years 1948–1952, 2001–2004, 2008–2009 and 2015–2017 are observable. This allows us to compute displacement rates over the three periods referred here as: Period 1 (second half of the 20th century), Period 2 (first decade of the 21st century) and Period 3 (Late 2000s to mid 2010s).

Aerial images have been regularly acquired by the IGN since the late 1940s, providing a valuable database for diachronic studies. This data source enables a significant increase in the temporal resolution of the analysis of the study sites. The aerial images are treated using the classic Structure from Motion (SfM) approach in Agisoft Photoscan[58]. Ground control point (GCPs) coordinates to georeference the model were acquired from a master frame, i.e. the 2018 UAV orthoimage (described in the section below) or the 2015–2017 IGN Orthoimage when UAV data is unavailable. GCPs are collected around the perimeter of the rock glacier to increase the accuracy of the resulting orthoimage within the landform area. The number of GCPs number is initially kept at its minimum for the georeferencing and optimisation process, i.e. three points, and increased if the resulting orthoimage does not present a suitable accuracy when compared to the master frame.

Because UAV photogrammetric missions are capable of providing high quality orthoimages and terrain models for rock glaciers[59,60], we conducted two surveys in summer-fall 2017 and 2018 at the PB, TL, RN and CL rock glacier sites. Images were acquired using the commercial UAV Mavick Pro and the automatic flight planner Drone Map. Except for the survey at PB in 2017, where the flight planner failed, all the surveys were conducted acquiring images with an overlap of 85% at an altitude of at least 90 m. For the 2018 session, a second flight level at 150 m altitude was added to the mission.

UAV pictures were treated using the classic SfM approach in Agisoft Photoscan. High precision GCPs were acquired only in 2018 using a Trimble GPS as a rover and a Trimble as a base. The method chosen was rapid-static and the raw data were post-processed in the differential mode. This allowed us to compute and georeference the DEMs and orthoimages for the 2018 survey and use their fixed areas as GCPs to reference the models from the 2017 surveys. This method was not used for the Longet rock glacier as the GCPs survey did not take place in 2018. At this site, the GCPs were measured from fixed areas in the available IGN orthoimage.

Data availability

The authors declare that the main data supporting the findings of this study are in Supplementary Data 1. These data, along with other additional files, are also available at the Pangaea repository database 'Rock glaciers in the French Alps—inventory of displacement rates and orthoimages of destabilized landforms—period 1945–2018'.

Code availability

The authors declare that the code used to obtain the main results of this study can be made available from the corresponding author upon request.

Received: 27 July 2020; Accepted: 11 March 2021;
Published online: 06 May 2021

References

1. Wahrhaftig, C. & Cox, A. Rock glaciers in the Alaska Range. *Geol. Soc. Am. Bull.* **70**, 383–436 (1959).
2. Jones, D. B., Harrison, S., Anderson, K. & Betts, R. A. Mountain rock glaciers contain globally significant water stores. *Sci. Rep.* **8**, 2834 (2018).
3. Amschwand, D., et al. Deciphering the evolution of the Bleis Marscha rock glacier (Val d'Err, eastern Switzerland) with cosmogenic nuclide exposure dating, aerial image correlation, and finite-element modelling. *The Cryosphere* https://tc.copernicus.org/preprints/tc-2020-209/ (2020).
4. Schoeneich, P., Bodin, X., Echelard, T. & Kaufmann, V. in *Engineering Geology for Society and Territory*, Vol. 1: Climate Change and Engineering Geology, pp. 223–227, https://doi.org/10.1007/978-3-319-09300-0_42 (Springer International Publishing Switzerland, 2015).
5. Haeberli, W. Creep of mountain permafrost: internal structure and flow of alpine rock glaciers. *Mitteilungen Der VAW/ETH Züric*, *77*. (1985).
6. Frehner, M. L., Mee Ling, A. H. & Gartner-Roer, I. Furrow-and-ridge morphology on rockglaciers explained by gravity-driven buckle folding: a case study from the murtèl rockglacier (Switzerland). *Permafr. Periglac. Process.* **26**, 57–66 (2015).
7. Wirz, V., Geertsema, M., Gruber, S. & Ross, S. Temporal variability of diverse mountain permafrost slope movements derived from multi-year daily GPS data, Mattertal, Switzerland. *Landslides* **13**, 67–83 (2016).
8. Bodin, X. et al. Two decades of responses (1986–2006) to climate by the Laurichard Rock Glacier, French Alps. *Permafr. Periglac. Process.* **344**, 331–344 (2009).
9. Shroder, J. F. Dendrogeomorphological analysis of mass movement on table cliffs plateau, Utah. *Quat. Res.* **9**, 168–185 (1978).
10. Scapozza, C. et al. Radiocarbon dating of fossil wood remains buried by the piancabella rock glacier, Blenio valley (Ticino, Southern Swiss Alps): Implications for rock glacier, treeline and climate history. *Permafr. Periglac. Process.* **21**, 90–96 (2010).
11. Sorg, A., Ka, A., Roesch, A., Bigler, C. & Stoffel, M. Contrasting responses of Central Asian rock glaciers to global warming. *Sci. Rep.* **5**, 8228 (2015).
12. Barsch, D. *Rockglaciers—Indicators of the Present and Former Geoecology in High Mountain Environments* (Springer-Verlag, 1996).
13. Kerschner, H., Ivy-Ochs, S. & Chlüchter, C. Paleoclimatic interpretation of the early late-glacial glacier in the Gschnitz valley, central Alps, Austria. *Ann. Glaciol.* **28**, 135–140 (1999).
14. Delaloye, R, et al. Recent Interannual Variations of Rock Glacier Creep in the European Alps. In *Proceeding of the Ninth International Conference on Permafrost*, 343–348, https://doi.org/10.5167/uzh-7031 (Fairbanks, Alaska, 2008).
15. Kellerer-Pirklbauer, A. & Kaufmann, V. Deglaciation and its impact on permafrost and rock glacier evolution: New insight from two adjacent cirques in Austria. *Sci. Total Environ.* **621**, 1397–1414 (2018).
16. Ikeda, A., Matsuoka, N. & Kääb, A. Fast deformation of perennially frozen debris in a warm rock glacier in the Swiss Alps: An effect of liquid water. *J. Geophys. Res. Earth Surf.* **113**, 1–12 (2008).
17. Buchli, T. et al. Kinematic investigations on the Furggwanghorn Rock Glacier, Switzerland. *Permafr. Periglac. Process.* **29**, 3–20 (2018).
18. Delaloye, R., Lambiel, C. & Gärtner-Roer, I. Overview of rock glacier kinematics research in the Swiss Alps. Seasonal rhythm, interannual variations and trends over several decades. *Geogr. Helv.* **65**, 135–145 (2010).
19. Cicoira, A., Beutel, J., Faillettaz, J., Gartner-Roer, I. & Vieli, A. Resolving the influence of temperature forcing through heat conduction on rock glacier dynamics: a numerical modelling approach. *The Cryosphere* **13**, 927–942 (2019).
20. Cicoira, A., Beutel, J., Faillettaz, J. & Vieli, A. Water controls the seasonal rhythm of rock glacier flow. *Earth Planet. Sci. Lett.* **528**, 115844 (2019).
21. Arenson, L. U. & Springman, S. M. Triaxial constant stress and constant strain rate tests on ice-rich permafrost samples. *Can. Geotech. J.* **42**, 412–430 (2005a).
22. Kääb, A., Frauenfelder, R. & Roer, I. On the response of rockglacier creep to surface temperature increase. *Glob. Planet. Change* **56**, 172–187 (2007).
23. Eriksen, H. Ø. et al. Recent acceleration of a Rock Glacier Complex, Ádjet, Norway, documented by 62 years of remote sensing observations. *Geophys. Res. Lett.* https://doi.org/10.1029/2018GL077605 (2018).
24. Kellerer-Pirklbauer, A. & Kaufmann, V. About the relationship between rock glacier velocity and climate parameters in central Austria. *Austrian J. Earth Sci.* **105**, 94–112 (2012).
25. Delaloye, R. et al. Rock glacier inventories and kinematics: a new IPA Action Group, in: 5th European Conference on Permafrost, Book of Abstract, 392–393. (Presented at the EUCOP5, Laboratoire EDYTEM, Chamonix, France, 2018).
26. Avian, M., Kaufmann, V. & Lieb, G. K. Recent and Holocene dynamics of a rock glacier system: The example of Langtalkar (Central Alps, Austria). Norsk *Geografisk Tidsskrift*, **59**, 149–156 (2005).
27. Bodin, X. et al. The 2006 Collapse of the Bérard Rock Glacier (Southern French Alps). *Permafr. Periglac. Process.* **28**, 209–223 (2016).
28. Delaloye, R. & Morard, S. Le glacier rocheux déstabilisé du Petit-Vélan (Val d ' Entremont, Valais) : morphologie de surface, vitesses de déplacement et structure interne, 3–5 (2011).

29. Delaloye, R. et al. Rapidly moving rock glaciers in Mattertal. *Jahrestagung Der Schweizerischen Geomorphologischen Gesellschaft* **29**, 21–31 (2013).
30. Lambiel, C. Le glacier rocheux déstabilisé de Tsaté-Moiry (VS):caractéristiques morphologiques et vitesses de déplacement. *La Géomorphologie Alpine: Entre Patimoine et Contrainte*, Géovisions n° 36. *Institut de géographie, Université de Lausanne* **3**, 5212–5224 (2011).
31. Roer, I., Haeberli, W., Avian, M., Kaufmann, V., Delaloye, R., Lambiel, C. & Kääb, A. Observations and considerations on destabilizing active rock glaciers in the European Alps. In *Proceedings of the 9th International Conference of Permafrost*, 1505–1510, https://doi.org/10.5167/uzh-6082 (Fairbanks, Alaska, 2008).
32. Scotti, R., Crosta, G. B. & Villa, A. Destabilisation of Creeping Permafrost: The Plator Rock Glacier Case Study (Central Italian Alps). *Permafr. Periglac. Process.* **28**, 224–236 (2016).
33. Cicoira, A. et al. A general theory of rock glacier creep based on in-situ and remote sensing observations. *Permafr. Periglac. Process.* https://doi.org/10.1002/ppp.2090 (2020).
34. Marcer, M. et al. Evaluating the destabilisation susceptibility of active rock glaciers in the French Alps. *The Cryosphere* **13**, 141–155 (2019).
35. Yamamoto, Y. & Springman, S. M. Three- and four-point bending tests on artificial frozen soil samples at temperatures close to 0 °C. *Cold Reg. Sci. Technol.* **134**, 20–32 (2017).
36. Mellor, M. & Testa, R. Effect of temperature on the creep of ice. *J. Glaciol.* **8**, 131–145 (1969).
37. Arenson, L. U. & Springman, S. M. Mathematical descriptions for the behaviour of ice-rich frozen soils at temperatures close to 0 °C. *Can. Geotech. J.* **42**, 431–442 (2005).
38. Arenson, L. U., Springman, S. M. & Sego, D. C. The rheology of frozen soils. *Appl. Rheol* **17**, 12147–1 (2006).
39. Kellerer-Pirklbauer, A. et al. Interannual variability of rock glacier flow velocities in the European Alps. In *Proceedings of the 5th European Conference on Permafrost*, 396–397 (Chamonix, France, 2018).
40. Kääb, A. et al. Inventory, motion and acceleration of rock glaciers in Ile Alatau and Kungöy Ala-Too, northern Tien Shan, since the 1950s. *Cryosphere Discuss.* **2020**, 1–37 (2020).
41. Marcer, M. et al. Permafrost favorability index: spatial modeling in the French Alps Using a Rock Glacier Inventory. *Front. Earth Sci.* **5**, 1–17 (2017).
42. Smith, M. W., Carrivick, J. L. & Quincey, D. J. Structure from motion photogrammetry in physical geography. *Prog. Phys. Geogr.* **40**, 247–275 (2016).
43. Holdsworth, G. Primary transverse crevasses. *J. Glaciol.* **8**, 107–129 (1969).
44. Durand, Y. et al. Reanalysis of 44 yr of climate in the French Alps (1958-2002): methodology, model validation, climatology, and trends for air temperature and precipitation. *J. Appl. Meteorol. Climatol.* **48**, 429–449 (2009).
45. Auer, I. et al. HISTALP – historical instrumental climatological surface time series of the Greater Alpine Region. *Int. J. Climatol.* **27**, 17–46 (2007).
46. Francou, B. & Reynaud, L. 10-year surficial velocities on a rock glacier (Laurichard, French Alps). *Permafr. Periglac. Process.* **3**, 209–213 (1992).
47. Thibert, E., Bonnefoy-Demongeot, M., Finance, F. & Bodin, X. Extracting the time signal in surface velocity changes along 3 decades at Laurichard rock glacier (French Alps), in: 5th European Conference on Permafrost, Book of Abstract. Presented at the EUCOP5, Laboratoire EDYTEM, Chamonix, France, 615–616 (2018).
48. Vaughan, D. G. Relating the occurrence of crevasses to surface strain rates. *J. Glaciol.* **39**, 255–266 (1993).
49. Colgan, W. et al. Glacier crevasses: observations, models, and mass balance implications. *Rev. Geophys.* **54**, 119–161 (2016).
50. Hosmer, D. & Lemeshow, S. *Applied Logistic Regression* (Wiley Interscience, 2000).
51. Kenner, R. et al. Factors controlling velocity variations at short-term, seasonal and multiyear time scales, ritigraben rock glacier, Western Swiss Alps. *Permafr. Periglac.Process.* **28**, 675–684 (2017).
52. Nickus, U. et al. Rock Glacier Äußeres Hochebenkar (Austria)—recent results of a monitoring network. *Zeitschrift für gletscherkunde und glazialgeologie* **47**, 43–62 (2013).
53. Vincent, C. Influence of climate change over the 20th century on four French glacier mass balances. *J. Geophys. Res.* **107**, 4375 (2002).
54. Huss, M., Funk, M. & Ohmura, A. Strong Alpine glacier melt in the 1940s due to enhanced solar radiation. *Geophys. Res. Lett.* **36**, 1–5 (2009).
55. GLAMOS. The Swiss Glaciers 2015/16 and 2016/2017. https://doi.org/10.18752/glrep 137–138 (2018).
56. Biskaborn, B. K. et al. Permafrost is warming at a global scale. *Nat. Commun.* **2019**, 1–11 (2019).
57. Kääb, A. & Vollmer, M. Surface geometry, thickness changes and flow fields on creeping mountain permafrost: Automatic extraction by digital image analysis. *Permafr. Perigla. Process.* **11**, 315–326 (2000).
58. Smith, M. W., Carrivick, J. L. & Quincey, D. J. Structure from motion photogrammetry in physical geography. *Prog. Phys. Geogr. Earth and Environ.* **40**, 247–275 (2016).
59. Vivero, S. & Lambiel, C. Monitoring the crisis of a rock glacier with repeated UAV surveys. *Geogr. Helv.* **74**, 59–69 (2019).
60. Dall'Asta, E. et al. Unmanned aerial systems and DSM matching for rock glacier monitoring. *ISPRS J. Photogramm. Remote Sens.* **127**, 102–114 (2017).

Acknowledgements

This study was funded by the European Regional Development Fund (POIA PA0004100) grant and by the French National Research Agency in the framework of the Investissements d'Avenir programs: Risk@UGA (ANR-15-IDEX). SAFRAN reanalysis data were provided by the CEN (Centre Etudes de le Neige), MétéoFrance Grenoble. The authors wish to thank Lucie Berenguer, Etienne Berthier, Samuel Morin and Baptiste Vandecrux, Robert Kenner, Adriano Ribolini and four anonymous reviewers for data treatment and for providing high quality feedback of the manuscript, improving the study.

Author contributions

P.S. and X.B. obtained the funding necessary to develop this study. M.M., A.C., X.B. and P.S. designed the study. M.M., D.C., T.E. and R.O. created the database of orthoimges and displacement rates. M.M. acquired field data and computed statistical analysis. M.M. and A.C. wrote the corpus of the study. All authors contributed in discussing and revising the analysis and findings.

Competing interests

The authors declare no competing interests.

Additional information

Supplementary information The online version contains supplementary material available at https://doi.org/10.1038/s43247-021-00150-6.

Correspondence and requests for materials should be addressed to M.M.

Peer review information Primary handling editor: Joe Aslin.

Reprints and permission information is available at http://www.nature.com/reprints

Publisher's note Springer Nature remains neutral with regard to jurisdictional claims in published maps and institutional affiliations.